Quantifying the momentum correlation between two light beams by detecting one

Armin Hochrainer[a,b,1], Mayukh Lahiri[a,b], Radek Lapkiewicz[a,b,2], Gabriela Barreto Lemos[a,b], and Anton Zeilinger[a,b,1]

[a]Institute for Quantum Optics and Quantum Information, Austrian Academy of Sciences, Vienna A-1090, Austria; and [b]Vienna Center for Quantum Science and Technology, Faculty of Physics, University of Vienna, Vienna A-1090, Austria

Contributed by Anton Zeilinger, December 20, 2016 (sent for review November 10, 2016; reviewed by Geraldo Barbosa and Zhe-Yu Ou)

We report a measurement of the transverse momentum correlation between two photons by detecting only one of them. Our method uses two identical sources in an arrangement in which the phenomenon of induced coherence without induced emission is observed. In this way, we produce an interference pattern in the superposition of one beam from each source. We quantify the transverse momentum correlation by analyzing the visibility of this pattern. Our approach might be useful for the characterization of correlated photon pair sources and may lead to an experimental measure of continuous variable entanglement, which relies on the detection of only one of two entangled particles.

quantum correlations | single-photon interference | complementarity principle | photon indistinguishability | photonic spatial modes

Spatial entanglement (1) of photon pairs plays an important role in fundamental quantum mechanics (2–4), quantum cryptography (5, 6), quantum teleportation (7), and quantum computation (8). A widely used strategy to test spatial entanglement is to directly measure intensity correlations in both near and far fields of the source plane, which are interpreted as correlations in the transverse positions and momenta of the two photons. Measurements of the transverse momentum correlation between two photons have been performed using a variety of experimental methods (3), including the scanning of two detectors (9, 10) or two slits (11), using detector arrays (12), spatial light modulators (13), and cameras (14). All of these methods rely on the detection of both of the correlated photons. This fact restricts their applicability to situations where the wavelength of both photons lies in a spectral range, for which sufficiently efficient detectors are available.

If two spatially separated nonlinear crystals emit pairs of photons (signal and idler) by the process of spontaneous parametric down conversion (SPDC) (15, 16), the two resulting signal beams in general do not interfere in lowest order (17). The absence of interference can be understood by the fact that the measurement on an idler photon would provide which-path information about a signal photon. However, lowest-order interference between the signal beams occurs if the respective idler beams are indistinguishable. This phenomenon, known as induced coherence without induced emission, was first observed experimentally in ref. 18, following a suggestion by Z.-Y. Ou of aligning the two idler beams (18, 19). The interferometric visibility is reduced if path-distinguishability is introduced via different transmissions (18, 19), different temporal delays (20), or different transverse sizes of the two idler beams (21, 22). Recently, the phenomenon led to applications in imaging (23), spectroscopy (24, 25), metrology (26), spectrum shaping (27), and fundamental tests of complementarity (e.g., refs. 28–30).

In this paper, we introduce and experimentally demonstrate a method for measuring the transverse momentum correlation between two photons by detecting only one of them. Our method is based on induced coherence without induced emission in a spatially multimode scenario. We produce an interference pattern in the signal beams generated by two identical sources that resembles fringes obtained in a Michelson interferometer. We show that the visibility of this pattern depends on the momentum correlation between signal and idler photons. We demonstrate how this dependence can be used to obtain quantitative information about the momentum correlation.

In our experiment (Fig. 1), two identical periodically poled nonlinear crystals (NL1 and NL2) are pumped coherently ($\lambda_p = 532$ nm) and emit photon pairs by collinear type-0 SPDC. The idler beam ($\lambda_i = 1{,}550$ nm) generated by NL1 is directed through NL2 to overlap with the idler beam produced at NL2. After NL2, the idler beam is discarded. The two signal beams ($\lambda_s = 810$ nm) are superposed at a beam splitter. The path lengths are chosen such that the detection of a signal or an idler photon yields no information from which of the two crystals it had emerged. Because the pump power is low (150 mW), we can neglect the probability of creating more than one photon pair at a time and thus the effect of stimulated emission (23, 31).

An EM CCD camera collects the superposed signal beam after it traverses a narrow-band (1 nm) frequency filter centered at 810 nm and a lens at focal distance from the camera. We assume the beams to be paraxial and the detection plane normal to the beam axis. In this case, the lens ensures that modes of the superposed signal beam with different transverse wave vectors $\mathbf{q}_s$ are detected at distinct points $\mathbf{r}_{\mathbf{q}_s} = \mathbf{q}_s(f_c\lambda_s/2\pi)$ on the camera.

Confocal lens systems (not in Fig. 1) ensure identical pump spots at NL1 and NL2 and point-by-point overlap of the idler beams. This arrangement causes each individual idler mode from NL1 to be indistinguishable from an equally populated idler mode

Significance

Entanglement as a fundamental concept of quantum physics is manifested in correlations between particles. The correlation between two particles is usually measured by detecting both of them. Here, we present the results of an experiment based on a unique concept, where the momentum correlation between two photons is measured by detecting only one of them. This measurement is possible by exploiting the quantum mechanical complementarity between path-distinguishability and interference. Our approach can potentially be generalized to measure other higher-order correlations in lower order, which would enable experimental access to a broader class of correlated quantum systems, particularly in situations in which technical limitations make it impossible to efficiently detect one of the correlated particles.

Author contributions: A.H., M.L., R.L., G.B.L., and A.Z. designed research, performed research, and wrote the paper.

Reviewers: G.B., QuantaSEC Consulting (present), Northwestern University (previous); and Z.-Y.O., Purdue University.

The authors declare no conflict of interest.

[1]To whom correspondence may be addressed. Email: anton.zeilinger@univie.ac.at or armin.hochrainer@univie.ac.at.

[2]Present address: Institute of Experimental Physics, Faculty of Physics, University of Warsaw, Pasteura 5, 02-093 Warsaw, Poland.

This article contains supporting information online at www.pnas.org/lookup/suppl/doi:10.1073/pnas.1620979114/-/DCSupplemental.

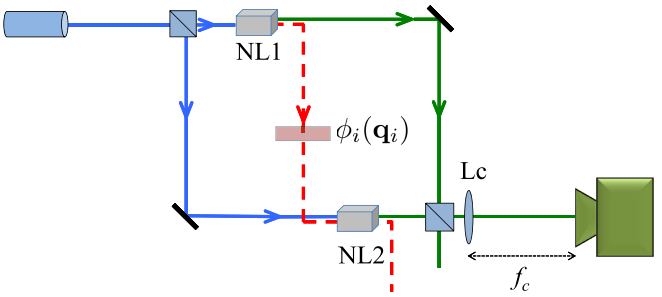

Fig. 1. Setup of the experiment. A continuous-wave pump laser (blue, 532 nm) is split at a beam splitter and focused into two identical nonlinear crystals (periodically poled potassium titanyl phosphate) NL1 and NL2. The crystals produce signal (green, 810 nm) and idler (red, 1,550 nm) photon pairs by type-0 SPDC. The idler beam from NL1 is overlapped with the idler beam from NL2 such that the two beams are indistinguishable after NL2. The two signal beams are superposed at a beam splitter, and a camera detects the output at the focal distance of a positive lens (Lc).

at NL2, and coherence between the respective signal modes is induced (23, 32). An additional lens system images the signal beam at NL1 to the equivalent plane of NL2, canceling the spatially dependent phase shift that would arise due to the relative propagation distance between of two signal beams. In this initial alignment position, the lens systems ensure a spatially uniform interferometric phase between the two interfering signal beams. If, however, plane wave modes of the idler beam with different transverse components acquire different phase shifts $\phi_i(\mathbf{q}_i)$ on their propagation from NL1 to NL2, the interference pattern in the superposed signal beam exhibits a spatial modulation.

It can be shown that the detected intensity pattern is given by (cf. ref. 33)

$$I(\mathbf{r}_{\mathbf{q}_s}) \propto P_s(\mathbf{q}_s) \int P(\mathbf{q}_i|\mathbf{q}_s)\,(1+\cos[\phi_i(\mathbf{q}_i)+\phi_0])\,d\mathbf{q}_i, \quad [1]$$

where ϕ_0 contains all phase terms that are constant across the beam cross-section. Here, $P(\mathbf{q}_i|\mathbf{q}_s) = P(\mathbf{q}_i,\mathbf{q}_s)/P_s(\mathbf{q}_s)$ describes the conditional probability density of detecting an idler photon with transverse momentum $\mathbf{p}_i = \hbar\mathbf{q}_i$ given that its partner signal photon has transverse momentum $\mathbf{p}_s = \hbar\mathbf{q}_s$. The variance $\Delta^2(\mathbf{p}_i|\mathbf{p}_s) = \hbar^2\Delta^2(\mathbf{q}_i|\mathbf{q}_s)$ corresponds to the range over which the momentum of an idler photon can vary, when the momentum of its partner signal photon is known (i.e., to the "width" of the correlation).

The visibility at each point on the interference pattern is evaluated by varying ϕ_0 and computing $v(\mathbf{r}_{\mathbf{q}_s}) = [I_{max}(\mathbf{r}_{\mathbf{q}_s}) - I_{min}(\mathbf{r}_{\mathbf{q}_s})]/[I_{max}(\mathbf{r}_{\mathbf{q}_s}) + I_{min}(\mathbf{r}_{\mathbf{q}_s})]$. It follows from Eq. **1** that for a given $\phi_i(\mathbf{q}_i)$, the visibility depends only on the conditional probability density $P(\mathbf{q}_i|\mathbf{q}_s)$. Therefore, under reasonable assumptions, the measured visibility can be used to determine $\Delta^2(\mathbf{q}_i|\mathbf{q}_s)$.

To analyze how the momentum correlation between signal and idler photons affects the visibility of the interference pattern, we first consider the case of perfectly anticorrelated transverse momenta, that is, $P(\mathbf{q}_i|\mathbf{q}_s) \propto \delta(\mathbf{q}_i + \mathbf{q}_s)$. In this case, it follows from Eq. **1** that the intensity at a particular point on the camera depends on the phase introduced on exactly one $\mathbf{q}_i$. As a result, the obtained interference pattern attains unit visibility.

On the other hand, if the momenta of signal and idler photons are uncorrelated, $P(\mathbf{q}_i|\mathbf{q}_s)$ is independent of $\mathbf{q}_s$. As a result, the interference pattern described by Eq. **1** exhibits no spatial modulation. In this case, the observed visibility can, in principle, still attain unity, if the introduced phase shift in the idler beam $\phi_i(\mathbf{q}_i)$ is constant for all $\mathbf{q}_i$. However, any variation of $\phi_i(\mathbf{q}_i)$ with $\mathbf{q}_i$ causes the camera to detect an average over infinitely many interference patterns, which are modulated by different phases. As a consequence, the visibility vanishes across the entire detected beam.

In general, the transverse momentum correlation between the two photons is neither perfect nor nonexistent, and $\Delta^2(\mathbf{q}_i|\mathbf{q}_s)$ is finite.

It follows from Eq. **1** that, in this case, phases acquired by several $\mathbf{q}_i$ contribute to the intensity modulation of the signal beam at one point on the camera. The range of contributing $\mathbf{q}_i$ is larger, the weaker the momenta of signal and idler photons are correlated. If $\phi_i(\mathbf{q}_i)$ is not constant for the $\mathbf{q}_i$ within that range, the visibility of the resulting fringes is reduced compared with the perfectly correlated case. This reduction of visibility is more pronounced if $\phi_i(\mathbf{q}_i)$ varies faster with $\mathbf{q}_i$ and if $\Delta^2(\mathbf{q}_i|\mathbf{q}_s)$ is larger. Therefore, the introduction of an inconstant $\phi_i(\mathbf{q}_i)$ is essential to determine $\Delta^2(\mathbf{q}_i|\mathbf{q}_s)$ with our method.

We introduced a spatially varying phase shift by translating a lens of the imaging system in the undetected idler beam between

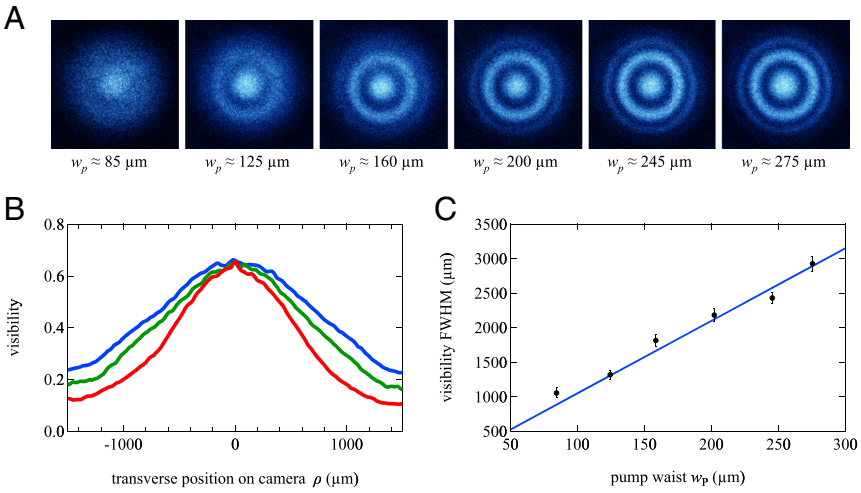

Fig. 2. Effect of a varying momentum correlation on the fringe visibility. Interference fringes are obtained in the signal beam by introducing an effective propagation distance (d = 11.7 mm) in the idler beam between the two crystals. (*A*) Examples of resulting camera images for different Gaussian pump waists w_P. Smaller w_P correspond to a weaker momentum correlation and to a lower visibility of the fringe pattern. (*B*) Visibility profiles evaluated from the data by scanning the relative phase in which the two crystals are pumped, for $w_P \approx 125$ μm (red), $w_P \approx 160$ μm (green) and $w_P \approx 200$ μm (blue). (*C*) Measured FWHM of the visibility as a function of the pump focus (black points) compared with a numerical simulation (blue line).

NL1 and NL2 along the optical axis. This phase shift is to a good approximation equivalent to a free-space propagation about a distance d (cf. ref. 34) and is given by

$$\phi_i(\mathbf{q}_i) = \frac{\lambda_i d}{4\pi}|\mathbf{q}_i|^2, \qquad [2]$$

where the distance was set to $d = 11.7$ mm in our experiment. The resulting interference pattern in the camera is circularly symmetric as the intensity value depends only on the radial distance ρ from the beam center. No spatially dependent phase was introduced in either of the detected signal beams.

The pump beam was focused equally into both crystals, subsequently using lenses of different focal lengths. The width of the momentum correlation was tuned by varying the size of the pump focus spots at NL1 and NL2 simultaneously (e.g., refs. 3 and 35). A narrow focus corresponds to more pump wave vectors contributing to the creation of down-converted photon pairs. The resulting uncertainty in transverse momentum of the pump beam leads to a weaker momentum correlation between signal and idler photons compared with cases, in which the pump beam is closer to collimation. Fig. 2*A* shows experimentally obtained interference patterns for different Gaussian pump waists w_p. In each pump configuration, the interferometric phase ϕ_0 was scanned. The visibility at each pixel on the camera was evaluated from the image data (*Supporting Information*). The obtained visibility profiles express a maximum value at the center of the interference pattern and decrease with the distance from the center. This behavior is expected, because the introduced quadratic phase $\phi_i(\mathbf{q}_i)$ varies faster for larger $\mathbf{q}_i$. Fig. 2*B* shows that a narrower pump focus corresponds to a faster decrease. The full width at half maximum (FWHM) of each visibility profile was determined. The results are presented in Fig. 2*C* in comparison with a numerical simulation.

To quantitatively relate our results to the variance of the transverse momentum correlation between signal and idler photons, the conditional probability density $P(\mathbf{q}_i|\mathbf{q}_s)$ needs to be parametrized. We assume that in the evaluated region of the beam, $P(\mathbf{q}_i|\mathbf{q}_s)$ can be approximated by a Gaussian distribution,

$$P(\mathbf{q}_i|\mathbf{q}_s) \propto \exp\left[-|\mathbf{q}_s + \mathbf{q}_i|^2/(2\sigma^2)\right], \qquad [3]$$

where the standard deviation σ represents a measure for how well the transverse momenta of signal and idler photons are correlated. This parameter is determined experimentally. Eq. **3** can be justified by comparison with the theoretical prediction for the SPDC emission in our experiment (*Supporting Information*). The resulting visibility can be explicitly calculated using Eqs. **1** and **2**.

A larger value of σ corresponds to a faster decrease of the visibility with the distance from the center. It can be shown that a one-to-one correspondence exists between the FWHM of the peak of the visibility profile and σ.* This fact allows to numerically compute the variance of the conditional transverse momentum distribution $\Delta^2(\mathbf{p}_i|\mathbf{p}_s) = \hbar^2\sigma^2$ from the measured FWHM values. Fig. 3 shows the results in comparison with the theoretical predictions.

In our approach, we circumvented the necessity of evaluating absolute visibility values, which is sensitive to experimental imperfections and noise.† Instead, we determined $\Delta^2(\mathbf{p}_i|\mathbf{p}_s)$ merely from relative visibility values obtained at different radial distances from the beam center on the camera.

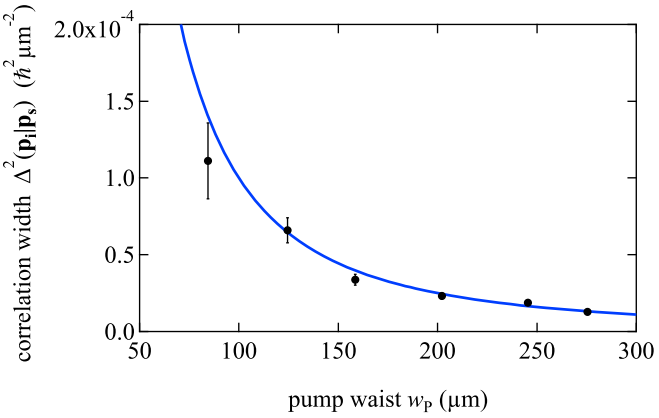

Fig. 3. Experimentally determined variance of the transverse momentum correlation between signal and idler photons ($\Delta^2(\mathbf{p}_i|\mathbf{p}_s) = \hbar^2\sigma^2$) for different Gaussian pump waists in both crystals. The black data points are obtained from measurements on signal photons only. The results are compared with the theoretical prediction, $\Delta^2(\mathbf{p}_i|\mathbf{p}_s) = \hbar^2/w_p^2$ (blue line).

We have demonstrated a method of quantifying the transverse momentum correlation between signal and idler photons by detecting only signal photons. Our method requires two sources, which have identical emission properties and emit photon pairs coherently. The latter is a necessary condition for the effect of induced coherence without induced emission to be observed. We assumed a specific Gaussian form of the conditional probability density of signal and idler transverse momenta. However, our approach could be easily extended to different distributions.

Experimentally, we determined the momentum correlation between two photons independently of their correlation in position. Previously, measurements of the spatial coherence of one beam have been used to show entanglement of biphotons under the assumption of pure states (see, for example, refs. 36–38). In our case, all measurements were performed in the momentum basis and we did not need to measure the spatial coherence of the signal beam. Furthermore, we did not perform any coincidence detection or post selection.

The presented method might be used for the characterization of sources of momentum correlated photons in situations where conventional methods involving coincidence detection are not practical (e.g., if detectors are not available for both wavelengths). From a fundamental viewpoint, our results demonstrate that it is possible to measure higher-order correlations between two systems without detecting one of them.

We believe that our method can be generalized to measure correlations not only in transverse momentum but also in transverse position and in other degrees of freedom. Such a generalization potentially has far-reaching implications in the characterization of spatially entangled states, because it opens a promising avenue of research toward an experimental measure of continuous-variable entanglement, which does not require a pure-state assumption and requires the detection of only one of two entangled particles.

ACKNOWLEDGMENTS. The authors thank F. Steinlechner for helpful discussions. This work was supported by the Austrian Academy of Sciences Institute for Quantum Optics and Quantum Information Vienna and Austrian Science Fund Special Research Programmes F40 (Foundations and Applications of Quantum Science) and W1210-2 (Complex Quantum Systems). R.L. was supported by Polish National Science Centre Grants 2015/17/D/ST2/03471 and 2015/16/S/ST2/00424.

*An explicit formula for the visibility in this situation is given by equation 22 in ref. 33. There, the quantity σ_θ is proportional to σ used in our treatment. It follows from this formula that the one-to-one correspondence holds in the regime of our interest.

†In fact, the absolute visibility at the center of the beam changes only minutely for the different values of w_P in our experiment. Moreover, the absolute visibility is very sensitive to alignment stability. We experimentally quantified the correlation via the FWHM, because this method relies only on relative visibilities and allows to robustly distinguish the obtained visibility profiles.

1. Einstein A, Podolsky B, Rosen N (1935) Can quantum-mechanical description of physical reality be considered complete? *Phys Rev* 47(10):777–780.
2. Horne MA, Shimony A, Zeilinger A (1989) Two-particle interferometry. *Phys Rev Lett* 62(19):2209–2212.
3. Walborn SP, Monken CH, Pádua S, Souto Ribeiro PH (2010) Spatial correlations in parametric down-conversion. *Phys Rep* 495(4–5):87–139.
4. Schneeloch J, Howell JC (2016) Introduction to the transverse spatial correlations in spontaneous parametric down-conversion through the biphoton birth zone. *J Opt* 18(5):053501.
5. Walborn SP, Lemelle DS, Almeida MP, Souto Ribeiro PH (2006) Quantum key distribution with higher-order alphabets using spatially encoded qudits. *Phys Rev Lett* 96(9):090501.
6. Walborn SP, Lemelle DS, Tasca DS, Souto Ribeiro PH (2008) Schemes for quantum key distribution with higher-order alphabets using single-photon fractional Fourier optics. *Phys Rev A* 77(6):062323.
7. Walborn SP, Ether DS, de Matos Filho RL, Zagury N (2007) Quantum teleportation of the angular spectrum of a single-photon field. *Phys Rev A* 76(3):033801.
8. Tasca DS, Gomes RM, Toscano F, Souto Ribeiro PH, Walborn SP (2011) Continuous-variable quantum computation with spatial degrees of freedom of photons. *Phys Rev A* 83(5):052325.
9. Pittman TB, Shih YH, Strekalov DV, Sergienko AV (1995) Optical imaging by means of two-photon quantum entanglement. *Phys Rev A* 52(5):R3429–R3432.
10. D'Angelo M, Kim Y-H, Kulik SP, Shih Y (2004) Identifying entanglement using quantum ghost interference and imaging. *Phys Rev Lett* 92(23):233601.
11. Howell JC, Bennink RS, Bentley SJ, Boyd RW (2004) Realization of the Einstein-Podolsky-Rosen paradox using momentum- and position-entangled photons from spontaneous parametric down conversion. *Phys Rev Lett* 92(21):210403.
12. O'Sullivan-Hale MN, Khan IA, Boyd RW, Howell JC (2005) Pixel entanglement: experimental realization of optically entangled d = 3 and d = 6 qudits. *Phys Rev Lett* 94(22):220501.
13. Hor-Meyll M, de Almeida JO, Lemos GB, Souto Ribeiro PH, Walborn SP (2014) Ancilla-assisted measurement of photonic spatial correlations and entanglement. *Phys Rev Lett* 112(5):053602.
14. Edgar MP, et al. (2012) Imaging high-dimensional spatial entanglement with a camera. *Nat Commun* 3:984.
15. Klyshko DN (1969) Scattering of light in a medium with nonlinear polarizability. *Sov Phys JETP* 28:522.
16. Burnham DC, Weinberg DL (1970) Observation of simultaneity in parametric production of optical photon pairs. *Phys Rev Lett* 25(2):84–87.
17. Hong CK, Ou ZY, Mandel L (1988) Interference between a fluorescent photon and a classical field: an example of nonclassical interference. *Phys Rev A Gen Phys* 37(8):3006–3009.
18. Zou XY, Wang LJ, Mandel L (1991) Induced coherence and indistinguishability in optical interference. *Phys Rev Lett* 67(3):318–321.
19. Wang LJ, Zou XY, Mandel L (1991) Induced coherence without induced emission. *Phys Rev A* 44(7):4614–4622.
20. Zou XY, Grayson T, Barbosa GA, Mandel L (1993) Control of visibility in the interference of signal photons by delays imposed on the idler photons. *Phys Rev A* 47(3):2293–2295.
21. Barbosa GA (1993) Degree of visibility in experiments of induced coherence without induced emission: a heuristic approach. *Phys Rev A* 48(6):4730–4734.
22. Grayson TP, Barbosa GA (1994) Spatial properties of spontaneous parametric down-conversion and their effect on induced coherence without induced emission. *Phys Rev A* 49(4):2948–2961.
23. Lemos GB, et al. (2014) Quantum imaging with undetected photons. *Nature* 512(7515):409–412.
24. Kulik SP, et al. (2004) Two-photon interference in the presence of absorption. *J Exp Theor Phys* 98(1):31–38.
25. Kalashnikov DA, Paterova AV, Kulik SP, Krivitsky LA (2016) Infrared spectroscopy with visible light. *Nat Photonics* 10:98–101.
26. Hudelist F, et al. (2014) Quantum metrology with parametric amplifier-based photon correlation interferometers. *Nat Commun* 5:3049.
27. Iskhakov TSh, et al. (2016) Nonlinear interferometer for tailoring the frequency spectrum of bright squeezed vacuum. *J Mod Opt* 63(1):64–70.
28. Herzog TJ, Kwiat PG, Weinfurter H, Zeilinger A (1995) Complementarity and the quantum eraser. *Phys Rev Lett* 75(17):3034–3037.
29. Heuer A, Menzel R, Milonni PW (2015) Induced coherence, vacuum fields, and complementarity in biphoton generation. *Phys Rev Lett* 114(5):053601.
30. Heuer A, Raabe S, Menzel R (2014) Phase memory across two single-photon interferometers including wavelength conversion. *Phys Rev A* 90(4):045803.
31. Wiseman HM, Mølmer K (2000) Induced coherence with and without induced emission. *Phys Lett A* 270(5):245–248.
32. Lahiri M, Lapkiewicz R, Lemos GB, Zeilinger A (2015) Theory of quantum imaging with undetected photons. *Phys Rev A* 92(1):013832.
33. Lahiri M, Hochrainer A, Lapkiewicz R, Lemos GB, Zeilinger A (2016) Twin photon correlations in single-photon interference. arXiv:1610.04298.
34. Hochrainer A, Lahiri M, Lapkiewicz R, Lemos GB, Zeilinger A (2016) Interference fringes controlled by non-interfering photons. arXiv:1610.05530.
35. Monken CH, Souto Ribeiro PH, Pádua S (1998) Transfer of angular spectrum and image formation in spontaneous parametric down-conversion. *Phys Rev A* 57(4):3123–3126.
36. Abouraddy AF, Nasr MB, Saleh BEA, Sergienko AV, Teich MC (2001) Demonstration of the complementarity of one- and two-photon interference. *Phys Rev A* 63(6):063803.
37. Di Lorenzo Pires H, Monken CH, van Exter MP (2009) Direct measurement of transverse-mode entanglement in two-photon states. *Phys Rev A* 80(2):022307.
38. Just F, Cavanna A, Chekhova MV, Leuchs G (2013) Transverse entanglement of biphotons. *New J Phys* 15(8):083015.
39. Grice WP, Bennink RS, Goodman DS, Ryan AT (2011) Spatial entanglement and optimal single-mode coupling. *Phys Rev A* 83(2):023810.
40. Tasca DS, Walborn SP, Souto Ribeiro PH, Toscano F, Pellat-Finet P (2009) Propagation of transverse intensity correlations of a two-photon state. *Phys Rev A* 79(3):033801.